

Received: 2019.02.02
Accepted: 2019.03.26
Published: 2019.07.20

Inhibitory Effects of Oxymatrine on Transdifferentiation of Neonatal Rat Cardiac Fibroblasts to Myofibroblasts Induced by Aldosterone via Keap1/Nrf2 Signaling Pathways *In Vitro*

Authors' Contribution:
Study Design A
Data Collection B
Statistical Analysis C
Data Interpretation D
Manuscript Preparation E
Literature Search F
Funds Collection G

ABCDEF 1,2,3 **Yu Yang***
ABCDE 1,2,3 **Shiping Chen***
ABCD 3 **Ling Tao**
ABCD 2,3 **Shiquan Gan**
ACD 2,3 **Hong Luo**
ACD 2,3 **Yini Xu**
ABCDFG 1,2,3 **Xiangchun Shen**

1 The Department of Pharmacognosy (The State Key Laboratory of Functions and Applications of Medicinal Plants, The High Educational Key Laboratory of Guizhou Province for Natural Medicinal Pharmacology and Druggability), School of Pharmaceutical Sciences, Guizhou Medical University, University Town, Guiyang, Guizhou, P.R. China
2 The Department of Pharmacology of Materia Medica (The High Efficacy Application of Natural Medicinal Resources Engineering Center of Guizhou Province, Union Key Laboratory of Guiyang City – Guizhou Medical University), School of Pharmaceutical Sciences, Guizhou Medical University, University Town, Guiyang, Guizhou, P.R. China
3 The Key Laboratory of Optimal Utilization of Natural Medicine Resources, School of Pharmaceutical Sciences, Guizhou Medical University, University Town, Guiyang, Guizhou, P.R. China

Corresponding Author:
Source of support:

* These authors contributed equally to this work and should be considered as co-first authors
Xiangchun Shen, e-mail: shenxiangchun@126.com

This work was supported by a grant from the National Natural Science Foundation of China (No. 81560588), the Key Project for Science and Technology Foundation of Guizhou Province (No. JZ-2015-2002), the Fund of High-Level Innovation Talents (No. 2015-4029), the Fund of Innovation Team of Guizhou Province (No. 2015-4025), the Fund of Innovated Team of the Education Department of Guizhou Province (No. 2014-31), the project of Administration of Traditional Chinese Medicine of Guizhou Province (No. QZYY-2018-086), the Foundation of Key Laboratory of Basic Pharmacology of Ministry of Education in Zunyi Medical University (No. QJHKY-2017-379), and the Basic Science Research Project of Guizhou Province (grant number [2019]1279)

Background: Oxymatrine (OMT), a quinolizidine alkaloid derived from the traditional Chinese herb *Radix Sophorae flavescens*, has widely reported pharmacological efficacy in treating cardiovascular dysfunction-related diseases. However, the underlying mechanism has been unclear. Here, we investigated the potential inhibitory effects and mechanism of OMT on transdifferentiation of cardiac fibroblast to myofibroblasts induced by aldosterone *in vitro*.

Material/Methods: The cardiac fibroblasts (CFBs) proliferation and migration capacity were evaluated by MTT assay, cell cycle assay, and scratch analysis, respectively. The protein expression of the Nrf2/Keap1 signal pathway, FN, Collagen I, Collagen III, α -SMA, CTGF, and mineralocorticoid receptor (MR) protein was detected by Western blot analysis. The mRNA expression of Nrf2 was detected by qRT-PCR. Immunofluorescence staining was used to observe the expression of α -SMA protein. Nrf2 siRNA was used to explore the role of Nrf2 in OMT-treated CFBs. GSH, SOD, and MDA levels and hydroxyproline content were measured by colorimetric assay with commercial kits. The DCFH-DA fluorescent probe was used to assess cellular ROS levels.

Results: OMT and Curcumin (an Nrf2 agonist) attenuated aldosterone (ALD)-induced proliferation and migration in CFBs, as well as the fibrosis-associated protein expression levels. Moreover, OMT activated Nrf2 and promoted the nucleus translocation of Nrf2. OMT alleviated the elevated levels of α -SMA, Collagen I, Collagen III, and CTGF, which were abrogated by the Nrf2 siRNA transfection. We also found that OMT decreased oxidative stress levels.

Conclusions: Our results confirm that OMT alleviates transdifferentiation of cardiac fibroblasts to myofibroblasts induced by aldosterone via activating the Nrf2/Keap1 pathway *in vitro*.

MeSH Keywords: **Aldosterone • Fibroblasts • NF-E2-Related Factor 2 • Reactive Oxygen Species**

Full-text PDF: <https://www.medscimonit.com/abstract/index/idArt/915542>



3641 6 44

Background

Cardiovascular diseases (CVDs) are major contributors to human morbidity and mortality worldwide [1]. Therefore, investigating the molecular mechanisms resulting in CVDs and discovering novel therapeutic agents have been the focus of research for many years [2]. It is well known that cardiac fibrosis is an important and common pathophysiological process in many cardiovascular diseases. Extensive cardiac fibrosis leads to increased ventricular stiffness, myocardial diastolic and systolic dysfunction, and ventricular arrhythmia, eventually resulting in heart failure and subsequent sudden death [3,4]. Cardiac fibroblasts (CFBs) play a critical part in the pathophysiology of cardiac fibrosis. Under pathological conditions, CFBs are activated by differentiation, migration, and proliferation [5]. Fibroblasts differentiated into myofibroblasts which characteristically express α -smooth muscle actin (α -SMA), secreted excessive extracellular matrix (ECM) proteins such as Collagen I, Collagen III, and fibronectin, and profibrotic factors such as connective tissue growth factor (CTGF). The imbalance between collagen synthesis and degradation in the ECM, which can lead to expansion of collagens, eventually results in myocardial fibrosis [6–8]. Therefore, it is critical to search for novel drugs that can suppress CFBs transdifferentiation and proliferation for prevention and clinical cure of cardiac fibrosis.

Emerging evidence shows that aldosterone (ALD), as an end signal molecule of the renin-angiotensin-aldosterone system, promotes ECM proteins expression, inducing fibrosis and participating in cardiac remodeling [9]. Specific binding of aldosterone with mineralocorticoid receptor (MR) promotes the progression of inflammation and cardiac fibrosis [10]. It is well known that excess oxidative stress and inflammation aggravate cardiac fibrosis [11,12]. Oxidative stress is a state characterized by dramatic generation of ROS relative to endogenous antioxidant ability. Abundant ROS production leads to ECM remodeling by irritating CFBs proliferation and activating matrix metalloproteinases (MMPs) [13]. Recently, nuclear factor-erythroid-2 (NF-E2-) related factor 2 (Nrf2) has been widely reported to be the main regulator of antioxidant response elements. Normally, Nrf2 is bound to Kelch-Like ECH-Associated Protein 1 (Keap1) in the cytoplasm. Nrf2 is separated from Keap1 after ROS production and is transferred into nucleus-bound antioxidant response elements (AREs), which initiate the transcription of heme oxygenase-1 (HO-1), and superoxide dismutase (SOD) inhibits the production of ROS [14,15].

Oxymatrine (OMT), a quinolizidine alkaloid derived from the traditional Chinese herb *Radix Sophorae flavescens*, exhibits various pharmacological activities [16], such as anti-tumor [17], anti-inflammation [18], anti-fibrosis [19], and cardio-protection action [20]. Previous data proved that OMT attenuates inflammation and renal fibrosis, probably via blocking the

TGF- β /Smad3 and NF- κ B p65 pathways. OMT significantly reduces fibronectin and collagen I expression [21]. OMT can attenuate CCl₄-induced hepatic fibrosis via modulation of TLR4-dependent inflammatory and TGF- β 1 signaling pathways [22]. Furthermore, recent evidence revealed that OMT can suppress the transdifferentiation and proliferation of CFBs induced by TGF- β [3,5]. In summary, there is abundant evidence suggesting that OMT has potential inhibitory effects on cardiac fibrosis.

It is well known that ALD is a strongly induced myocardial fibrosis factor in the heart. Here, we investigated the effect of OMT on the anti-fibrosis effect induced by ALD and explore its potential mechanism via Nrf2 signaling.

Material and Methods

Ethics statement

All animal experiments conformed to the Guide for the Care and Use of Laboratory Animals published by Guizhou Medical University and were approved by the Committee for Experimental Animal Ethics of Guizhou Medical University [No. 1503068].

Materials and reagents

OMT (purity, 98%) was purchased from Nanjing Guangrun Biotechnology Co., Nanjing, China. ALD (purity, 95%) and curcumin (purity, 98%) were from Sigma, USA. Spironolactone (purity, 99%) was purchased from Jinglai Biological, China. Dulbecco's modified Eagle's medium (DMEM) was purchased from GIBCO (Gaithersburg, USA). Malondialdehyde (MDA), Glutathione (GSH), Superoxide dismutase (SOD), and Hydroxyproline commercial kits were purchased from Jiancheng Bioengineering (Nanjing, China). Cell Cycle Detection kits were obtained from KeyGEN BioTECH (Nanjing, China). Vimentin, Collagen I, Nrf2, Keap1, HO-1, α -SMA, Fibronectin, Tubulin, LaminB1, MR, and GAPDH antibodies were obtained from Proteintech, USA. Collagen III and CTGF antibodies were purchased from Medical Discovery Leader, China. Nrf2-siRNA was purchased from GenePharma Shanghai, China. Reactive oxygen species (ROS) Assay kits were obtained from Yeasen Biotech Co., Shanghai, China.

Culture and treatment of primary cardiac fibroblasts (CFBs)

CFBs were isolated and purified from cardiac tissues of 1- to 2-days-old Sprague-Dawley rats using continuous enzyme digestion with 0.08% trypsin, and were plated on culture flasks, as previously described [2,5]. Briefly, the enzymatically separated cells were suspended in DMEM containing 12% fetal bovine serum (FBS), plated on culture flasks, harvested, and purified by 90-min

differential adherence. The primary CFBs were cultured with DMEM containing 12% fetal bovine serum at 37°C in an atmosphere of 5% CO₂. The second-passage CFBs were used for subsequent experiments. The purity of cultured CFBs was assessed through immunocytochemistry staining using mouse monoclonal vimentin antibody. The CFBs were cultured to approximately 80% confluence, and then incubated in serum-free DMEM for 24 h. Cultured CFBs were exposed to aldosterone (0.1 μmol/L) alone for 24 h, or pre-incubated with curcumin (10 μmol/L), Spironolactone (Spiro) (1 μmol/L), OMT-L (18.9 μmol/L), and OMT-H (37.8 μmol/L) for 2 h, then exposed to ALD treatment for 24 h.

CFBs proliferation assay

MTT (5 mg/mL) was added into 96-well plates in the dark at designated experimental timepoints. After incubation for 4 h at 37°C in a 5% CO₂ incubator, the formazan crystals were dissolved in 150 μL DMSO, and then the absorbance values were detected at 490 nm by using a microplate reader (ELX800; General Electric, Fairfield, CT).

Giemsa staining

At the designated timepoints, cells were fixed with 4% paraformaldehyde for 20 min, and then washed 3 times with PBS, stained with Giemsa dye (Baso Bioscience) A and B for 10 min, and the cellular morphology was imaged using a microscope.

Immunofluorescence staining

The CFBs were plated on 24-well plates. At the designated timepoints, cells were fixed with 4% paraformaldehyde for 20 min, permeabilized with 0.5% Triton X-100 for 20 min, blocked in 7.5% goat serum for 1 h at room temperature, and then CFBs were incubated with a rabbit polyclonal anti-α-SMA primary antibody (1: 50 dilution) at 4°C overnight. Next, (FITC-conjugated goat anti-rabbit IgG, 1: 100 dilution) antibodies were incubated for 1 h at room temperature and counterstained with DAPI (5 mg/mL) for 10 min. All images were captured using a fluorescence microscope (Nikon Corporation, Tokyo, Japan).

Scratch experiment

The migration capacity of CFBs was evaluated by scratch assay as previously described [2,5]. Briefly, The CFBs were plated on 6-well plates and grown to about 90% confluence. An artificial gap was generated by scratching with a sterile pipette tip. The width of the gap was measured at 24 h intervals.

Hydroxyproline colorimetric assay

The level of hydroxyproline (Hyp) in supernatant of CFBs was determined using a commercial Hyp detection kit. OD values

of samples were detected by microplate reader, and then the level of Hyp was calculated in accordance with the manufacturer's instructions.

Cell cycle assay

Cell cycle was assayed using flow cytometry. The CFBs were collected after treatment and fixed overnight with 70% ethanol at 4°C, according to the manufacturer's protocols, and the results were assessed using ACEA NovoCyte. Data were analyzed using NovoExpress software.

Transfection of CFBs with Nrf2 siRNA

The sequence of the rat Nrf2 siRNA was 5'-GCAGCAUACAGCAG GACAUTT-3', and its complementary strand was 5'-AUGUCCUGCUGU AUGCUGCTT-3'. According to the manufacturer's instructions, the CFBs were transfected with 50 nM Nrf2-siRNA or negative control siRNA (NC) with Lipofectamine 2000 (Invitrogen) for 24 h. Transfected cells were subjected to ALD alone for 24 h, or pre-incubation with OMT for 2 h before being subjected to ALD for 24 h. Western blot analysis was performed to assess the silencing effect.

Measurement of intracellular reactive oxygen species in CFBs

The level of intracellular reactive oxygen species (ROS) was measured with 2',7'-dichlorofluorescein diacetate (DCFH-DA). Briefly, after different treatments, CFBs were incubated with 10 μM DCFH-DA for 30 min at 37°C. Then, intracellular ROS was detected by immunofluorescence microscope and the OD value was also checked by fluorometer (VLBLOT2, Thermo Fisher Scientific, Vantaa, Finland).

Measurement of the levels of malondialdehyde (MDA) and glutathione (GSH), and superoxide dismutase (SOD) activity

The levels of intracellular MDA and GSH, and SOD activity in CFBs were detected by MDA, SOD, and GSH commercial kits, according to the manufacturer's protocols. The results were calculated according to the manufacturer's instructions.

Western blot analysis

At the designated timepoints, CFBs protein was extracted using RIPA buffer with protease and phosphatase inhibitors. The nuclear and cytoplasmic protein was extracted using nuclear and cytoplasmic protein extraction kits (Bestbio Institute of Biotechnology), according to the manufacturer's protocols. The BCA protein detection kit was used to measure the protein concentration. Equivalent amounts of protein samples

(20–30 µg) were fractionated by sodium dodecyl sulfate-polyacrylamide gel electrophoresis (SDS-PAGE) on an 8% gel and subsequently transferred to polyvinylidene difluoride (PVDF) membranes at 4°C, then blocked with 5% non-fat milk in TBST at room temperature for 2 h. The membranes were incubated with the following primary antibody at 4°C overnight: α -SMA (14395-1-AP, Proteintech, 1: 1000), Fibronectin (66042-1-Ig, Proteintech, 1: 5000), CTGF (MD5912-50, Medical Discovery Leader, 1: 1000), Collagen III (MD4405-50, Medical Discovery Leader, 1: 1000), HO-1(66743-1-Ig, Proteintech, 1: 1000), and Nrf2 (16396-1-AP, Proteintech, 1: 1000), Keap1(10503-2-AP, Proteintech, 1: 1000), collagen I (14695-1-AP, Proteintech, 1: 1000), MR (21854-1-AP, Proteintech, 1: 1000), LaminB1 (12987-1-AP, Proteintech, 1: 1000), Tubulin (10094-1-AP, Proteintech, 1: 10,000) and GAPDH (60004-1-Ig, Proteintech, 1: 10000). After washing the membranes 3 times with 1×TBST, the membranes were incubated for 1.5 h at room temperature with Anti-mouse IgG (1: 10 000, PMK-014-095) and Anti-rabbit IgG (1: 10 000, PMK-014-090). The antigen-antibody complexes were detected by enhanced chemiluminescence (ECL, 7Sea Biotechnology, Shanghai, China). Bands were scanned and quantified using Syngene Gel Imaging System (Bio-Rad) analysis software.

RNA extraction and quantitative real-time polymerase chain reaction (qRT-PCR)

Total cellular RNA was extracted from CFBS using the E.Z.N.A.[®] Total RNA kit I (R6834-01, OMEGA) according to the manufacturer's instructions. RNA was reverse-transcribed into cDNA using the PrimeScript[™] RT reagent kit (RR037A, Takara Bio, Inc.). Quantitative real-time PCR was performed on cDNA using SYBR[®] Premix Ex Taq[™] II (Takara Bio, Inc.) and the CFX Manager 3.0 Real-Time PCR System (Bio-Rad). GAPDH was used as the internal control for mRNA expression. The specific primers used were as follows: rat Nrf2 forward, 5'-GCCTCCTCTGCTGCCATTAGTC-3', and reverse, 5'-TCATTGAACTCCACCGTGCCTTC-3'; rat GAPDH, forward, 5'-GACATGCCCGCTGGAGAAAC-3, reverse, 5'-AGCCCAGGATGCCCTTGTAGT-3'.

Statistical analysis

All data are expressed as the mean \pm SEM. All data analysis was performed using GraphPad prism[®] 6.0 software (La Jolla, CA). Statistical analysis was performed using one- or two-way ANOVA for multiple comparisons and the *t* test for 2 groups. A value of *P*<0.05 was considered to be statistically significant. Data were derived from at least 3 independent experiments.

Results

OMT inhibits proliferation in CFBS subjected to ALD

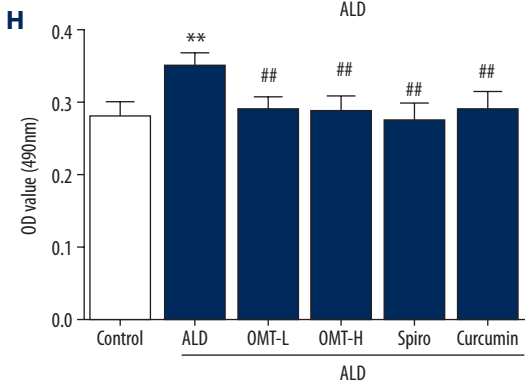
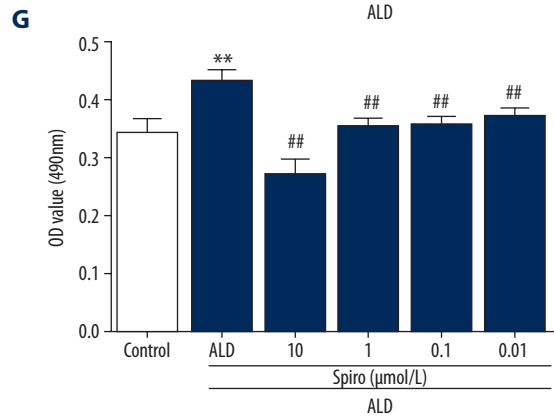
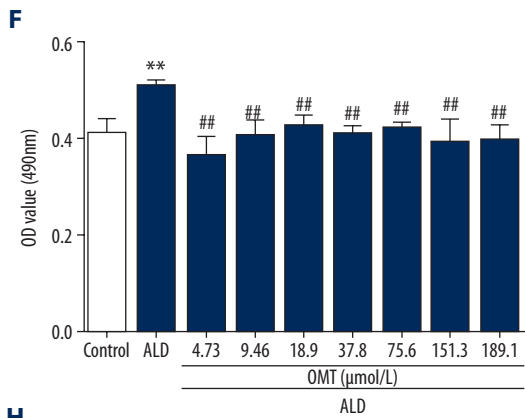
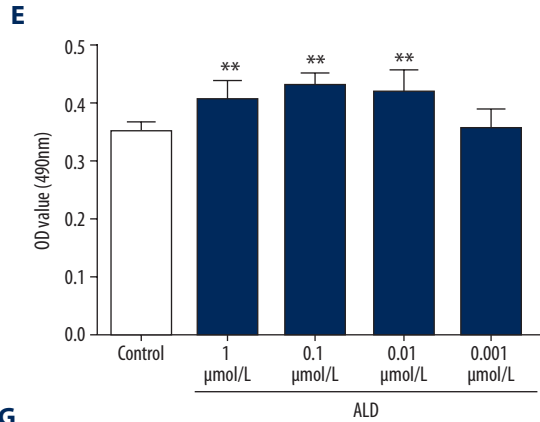
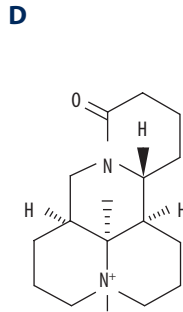
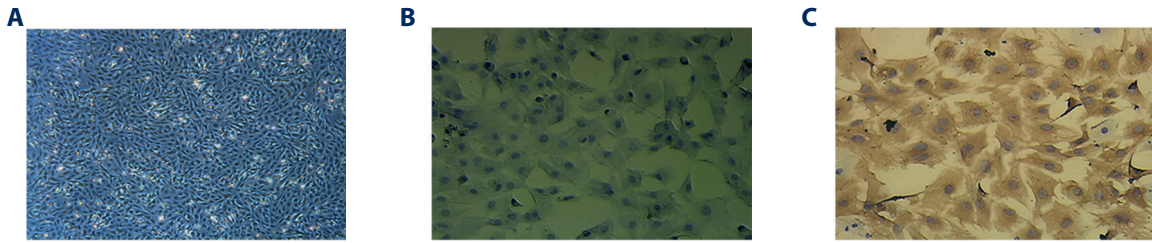
The primary CFBS were mostly thin and triangular-shaped, as shown by use of an inverted microscope (Figure 1A). Vimentin, the specific biomarker of mesenchymal cells, was used to identify CFBS. The purity of cultured CFBS was more than 95% by immunocytochemistry (Figure 1B, 1C). The OMT chemical structure is shown in Figure 1D. The concentrations of ALD, OMT, and spironolactone were determined by MTT assay and previous data. CFBS were treated with different concentrations of ALD (0.001–1 µmol/L) for 24 h. The results showed that 0.1 µmol/L ALD significantly promoted cell proliferation (Figure 1E). Then, CFBS were pre-incubated with various concentrations of OMT (4.73–189.1 µmol/L) and spironolactone (0.01–10 µmol/L) for 2 h before being subjected to ALD for 24 h. The results showed that OMT (18.9 µmol/L, 37.8 µmol/L) and spironolactone (1 µmol/L) inhibited ALD-induced cell proliferation of CFBS (Figure 1F, 1G), in agreement with previous reports [5,23]. Figure 1H shows that, compared to the control group, ALD significantly increased CFBS proliferation. Pre-incubated with OMT, the MR antagonist spironolactone, and the Nrf2 agonist curcumin inhibited this proliferation effect displayed by MTT. ALD exposure remarkably increased the number of CFBS compared to the control group, which was attenuated by pre-incubation with OMT, spironolactone, and curcumin (Figure 1I) as shown by Giemsa staining. Taken together, these data suggest that OMT and curcumin can ameliorate ALD-induced CFBS proliferation.

Effect of OMT on the cell cycle and migration ability of CFBS induced by ALD

After exposure of CFBS to ALD, S phase was significantly increased compared to the control group. Pretreatment with OMT, spironolactone, and curcumin inhibited the number of cells in S phase of the cell cycle following ALD stimulation (Figure 2A, 2B). As shown in Figure 2C and 2D, the scratch results showed that ALD exposure enhanced migration ability of CFBS. Pre-incubation with OMT, spironolactone, and curcumin significantly alleviated the migration ability of CFBS induced by ALD (Figure 2C, 2D).

OMT inhibited ALD-induced hydroxyproline (Hyp) secretion and Collagen I, Collagen III, FN, α -SMA, CTGF, and MR expression of CFBS

Hydroxyproline (Hyp), a biomarker of collagen secretion, is a degradation product of collagen. After exposure to ALD, the Hyp content was significantly increased in medium. OMT, spironolactone, and curcumin significantly alleviated the ALD-induced Hyp secretion (Figure 3A). The expression levels



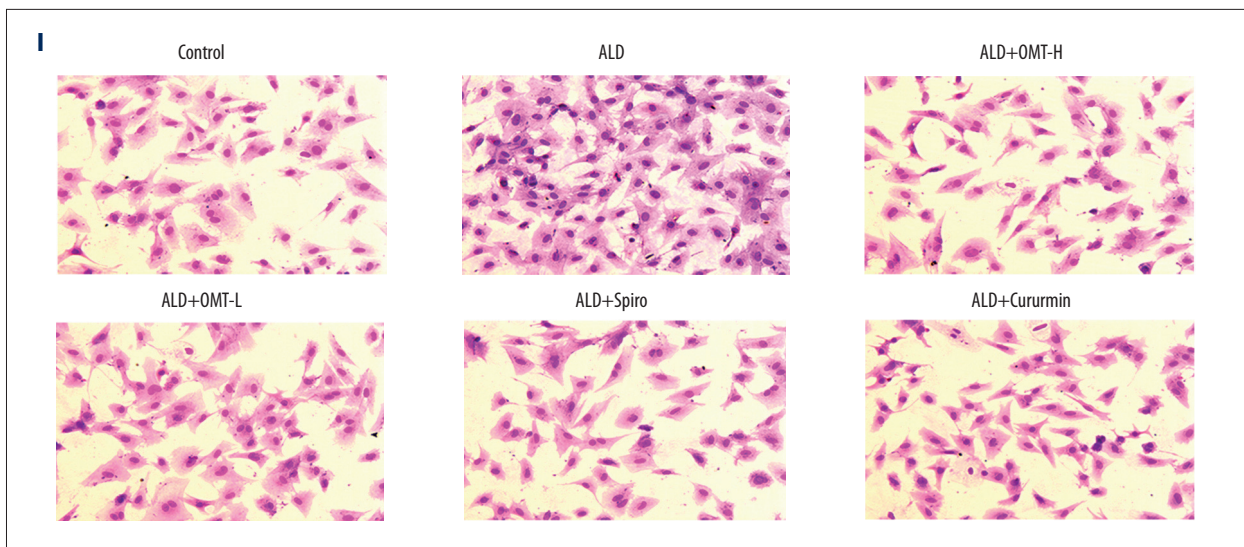


Figure 1. OMT and curcumin inhibit ALD-induced proliferation in CFBs. **(A)** Morphology image of the primary CFBs (magnification, 50 \times). **(B)** Representative image of negative control stained cells (PBS was used instead of primary antibody, magnification, 200 \times). **(C)** Representative image of cells stained with the anti-vimentin antibody (magnification, 200 \times). **(D)** The OMT chemical structure. **(E)** Effects of various concentrations of ALD (0.001–1 $\mu\text{mol/L}$) on proliferation of CFBs. **(F)** Effects of various concentrations of OMT (4.73–189.1 $\mu\text{mol/L}$) on ALD-induced proliferation of CFBs. **(G)** Effects of various concentrations of spironolactone (0.01–10 $\mu\text{mol/L}$) on ALD-induced proliferation of CFBs. **(H)** CFBs were pretreated with 10 $\mu\text{mol/L}$ curcumin, 1 $\mu\text{mol/L}$ spironolactone (Spiro), 18.9 $\mu\text{mol/L}$ OMT, or 37.8 $\mu\text{mol/L}$ OMT for 2 h, and then exposed to 0.1 $\mu\text{mol/L}$ ALD for 24 h. The MTT assay was used to measure cell viability. **(I)** CFBs morphological change revealed by Giemsa staining analysis. Cytoplasm was stained pink and nucleus stained violet (magnification, 200 \times). Results are presented as the mean \pm SEM (* $p < 0.05$ and ** $p < 0.01$ vs. control; # $p < 0.05$ and ## $p < 0.01$ vs. ALD).

of fibrosis-associated proteins of Collagen I, Collagen III, FN, α -SMA, CTGF, and MR were remarkably increased induced by ALD compared to the control group (Figure 3B–3H). OMT attenuated the proteins of ALD-induced Collagen I, Collagen III, FN, α -SMA, CTGF, and MR, as well as spironolactone and curcumin (Figure 3B–3H). A similar trend was confirmed in immunofluorescent staining for α -SMA by fluorescence microscopy (Figure 3I).

OMT ameliorated ALD-induced cardiac fibrosis via activating the Nrf2/Keap1 pathway

The protein of Nrf2 and Keap1 in cytoplasm expression contents were remarkably increased in the ALD group as shown by Western blot assay (Figure 4B, 4C). OMT, spironolactone, and curcumin attenuated the protein levels of ALD-induced Nrf2 and Keap1 protein in cytoplasm (Figure 4B, 4C). After exposing CFBs to ALD, the expression of Nrf2 in the nucleus and HO-1 were significantly decreased compared with the control group (Figure 4A, 4D), which were reversed by OMT, spironolactone, and curcumin (Figure 4A, 4D). The Nrf2 protein in cytoplasm, Keap1 in cytoplasm, HO-1, and Nrf2 in the nucleus exhibited no significant difference between the curcumin group and the OMT + curcumin group (Figure 4A–4D). Furthermore, pretreatment with OMT, spironolactone, and curcumin also increased the ALD reduced Nrf2 mRNA expression (Figure 4E).

As shown in Figure 5A, 5B, the transfection efficiency of Nrf2 siRNA was more than 60%. OMT significantly decreased ALD-induced upregulation of α -SMA, a common biomarker for fibroblast-to-myoblast transdifferentiation. However, the ameliorated effect of OMT was reversed by Nrf2 siRNA. The α -SMA protein expression exhibited no significant difference between the Nrf2 siRNA groups and OMT+Nrf2 siRNA groups (Figure 5C, 5D), which means that OMT depends on the Nrf2 signal pathway. A similar trend was confirmed in immunofluorescent staining for α -SMA by fluorescence microscopy (Figure 5H). As shown in Figure 5E–5G, the results illustrated that the upregulated levels of CTGF, collagen I, and collagen III induced by ALD exposure were significantly decreased by OMT, and Nrf2 siRNA abolished this trend. The collagen I, collagen III, and CTGF protein expression exhibited no significant difference between the Nrf2 siRNA groups and the OMT+Nrf2 siRNA groups (Figure 5E–5G).

OMT inhibits oxidative stress levels in CFBs induced by ALD

It is well known that oxidant stress participates in the activation of CFBs and differentiation of CFBs into myofibroblasts. In the present study, ROS contents were detected by fluorescent probe DCFH-DA and we also detected the relative fluorescence intensity (OD value). As shown in Figure 6A, 6B, the relative

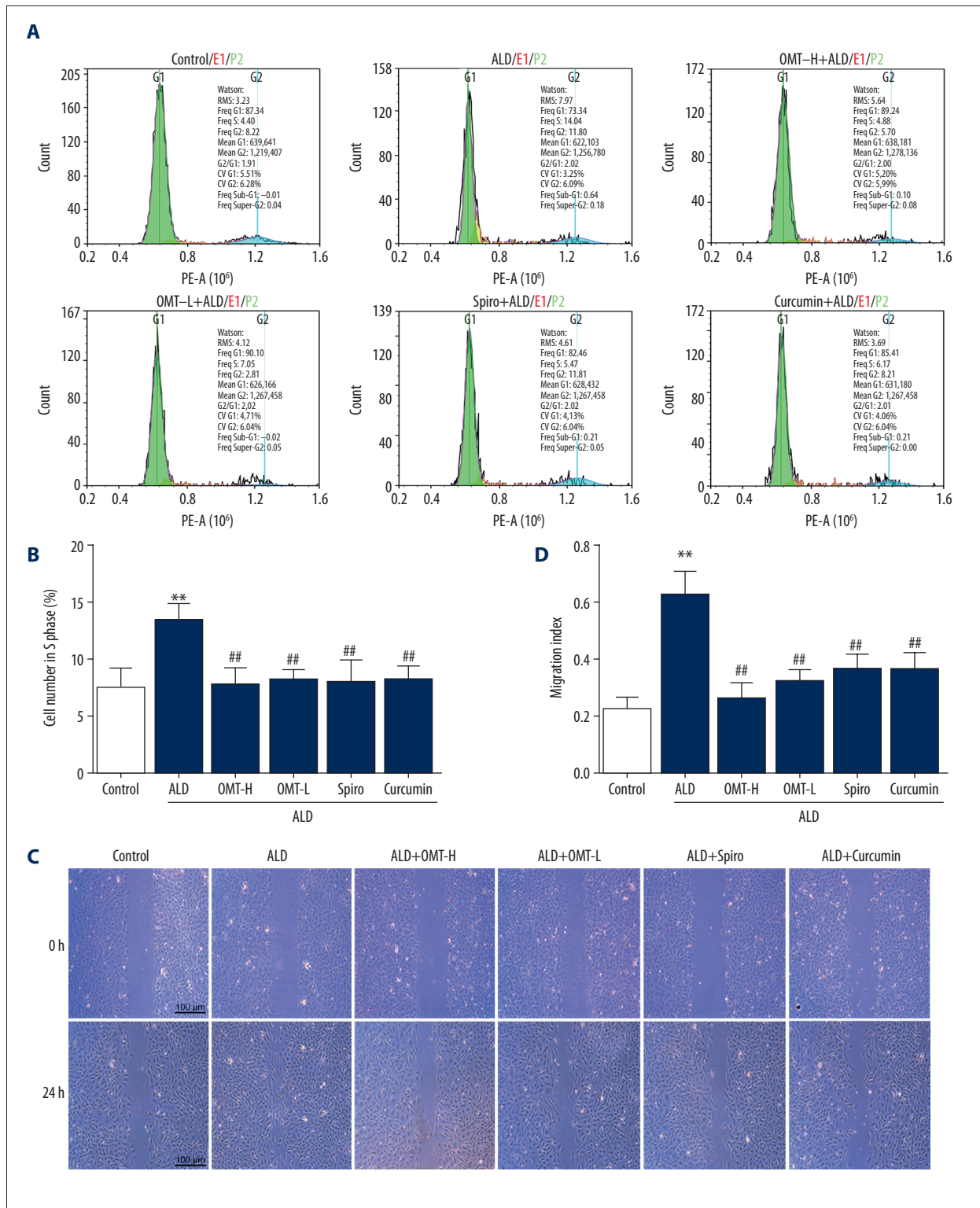


Figure 2. Effect of OMT and curcumin on the cell cycle and migration ability of CFBs induced by ALD. CFBs were pretreated with 10 $\mu\text{mol/L}$ curcumin, 1 $\mu\text{mol/L}$ spironolactone (Spiro), 18.9 $\mu\text{mol/L}$ OMT, or 37.8 $\mu\text{mol/L}$ OMT for 2 h, and then exposed to 0.1 $\mu\text{mol/L}$ ALD for 24 h. (**A**, **B**) Flow cytometry was used to assess cell cycle. (**C**, **D**) Quantification of the width of cell migration after scratch test. Results are presented as the mean \pm SEM (* $p < 0.05$ and ** $p < 0.01$ vs. control; # $p < 0.05$ and ## $p < 0.01$ vs. ALD).

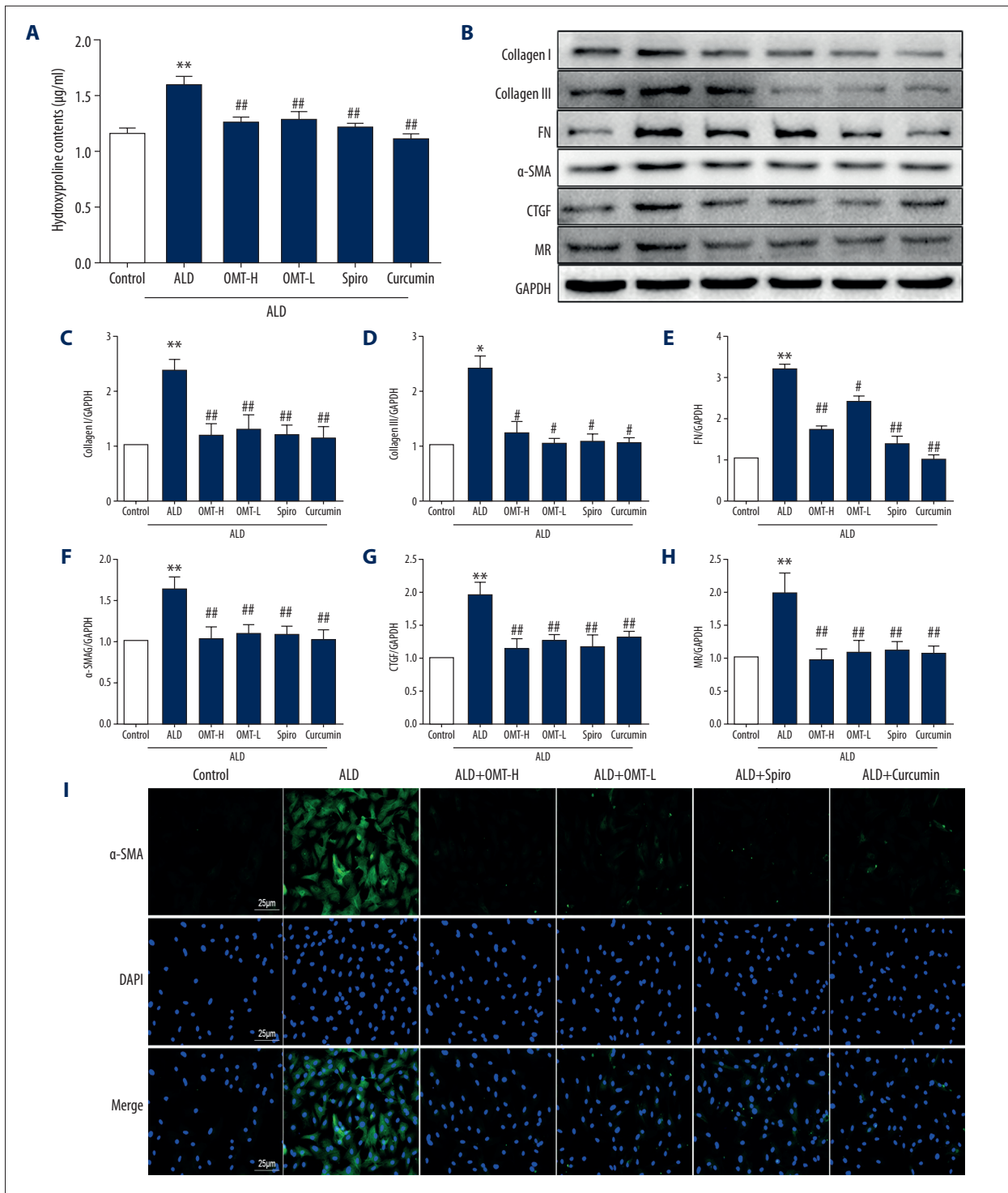


Figure 3. Effects of OMT and curcumin on Collagen I, Collagen III, FN, α-SMA, CTGF, and MR induced by ALD in CFBs. CFBs were pretreated with 10 µmol/L curcumin, 1 µmol/L spironolactone (Spiro), 18.9 µmol/L OMT, or 37.8 µmol/L OMT for 2 h, and then exposed to 0.1 µmol/L ALD for 24 h. (A) The expression of hydroxyproline content in CFBs supernatant was determined using a commercial kit. Western blot was used to assess expression of (B, C) Collagen I, (D) Collagen III, (E) FN, (F) α-SMA, (G) CTGF, and (H) MR protein in CFBs. (I) Immunofluorescent staining for α-SMA (green) and nuclear marker DAPI (blue) in CFBs after indicated treatment (magnification, 200×). Results are presented as the mean ±SEM (* p<0.05 and ** p<0.01 vs. control; # p<0.05 and ## p<0.01 vs. ALD).

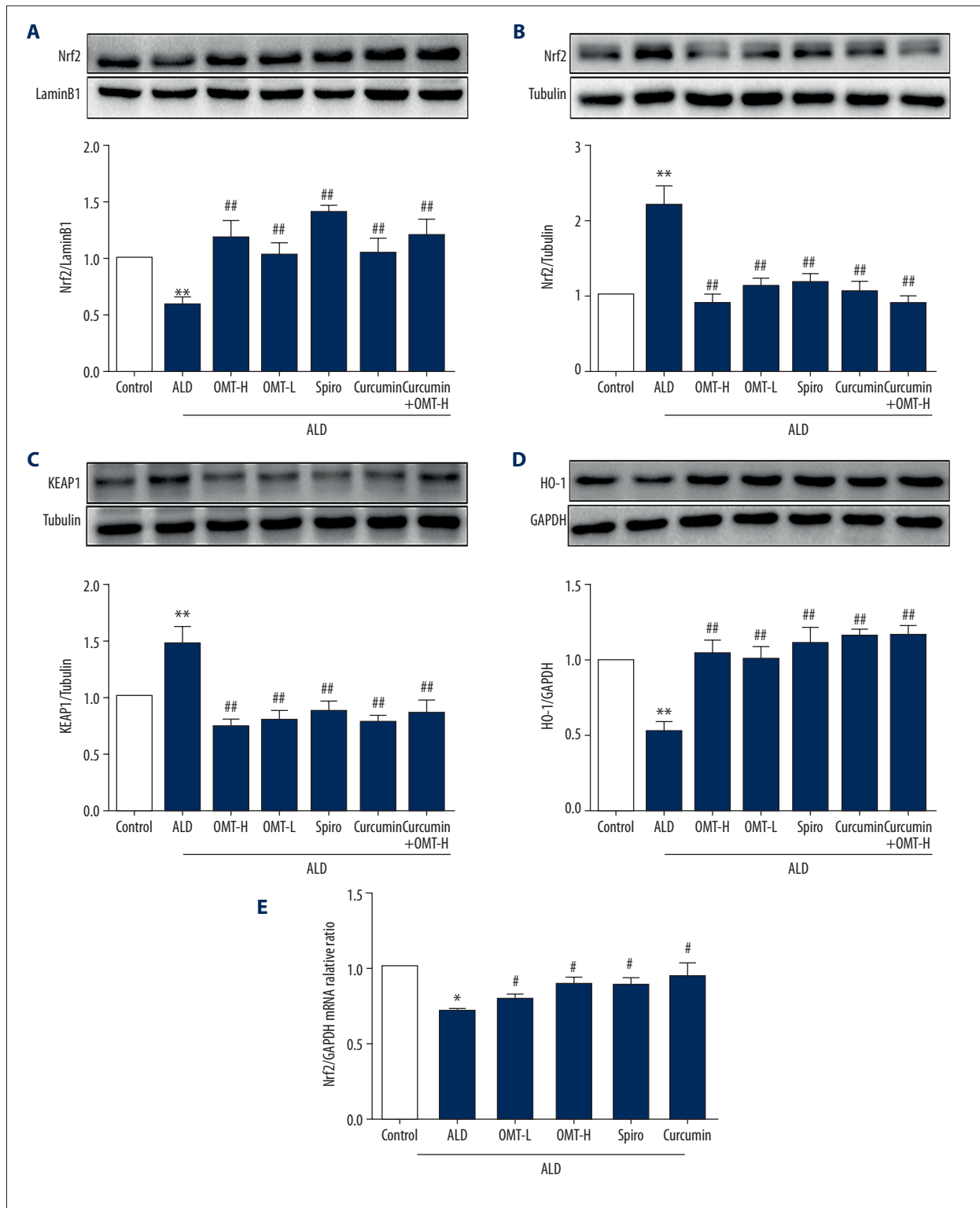


Figure 4. OMT ameliorating ALD-induced cardiac fibrosis is involved in the Nrf2/Keap1 signaling pathway. CFBs were pretreated with 10 $\mu\text{mol/L}$ curcumin, 1 $\mu\text{mol/L}$ spironolactone (Spiro), 18.9 $\mu\text{mol/L}$ OMT, or 37.8 $\mu\text{mol/L}$ OMT for 2 h, and then exposed to 0.1 $\mu\text{mol/L}$ ALD for 24 h. Western blot analysis of (A) Nrf2 in nuclear, (B) Nrf2 in cytosolic, (C) Keap1 in cytosolic, and (D) HO-1 protein expression of CFBs. (E) qRT-PCR analysis of the relative mRNA levels of Nrf2 in different groups. Results are presented as the mean \pm SEM (* $p < 0.05$ and ** $p < 0.01$ vs. control; # $p < 0.05$ and ## $p < 0.01$ vs. ALD).

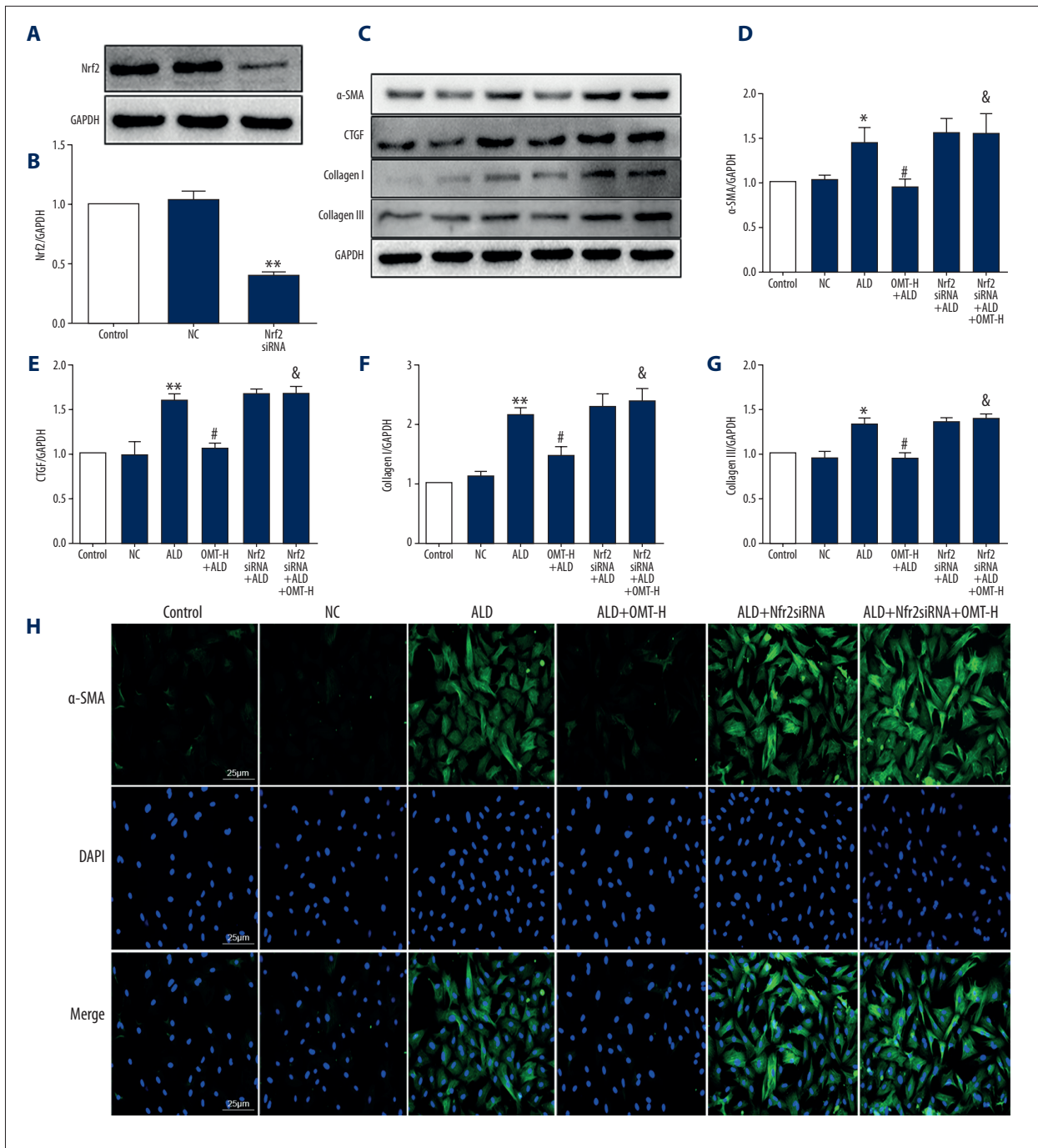


Figure 5. OMT inhibited ALD-induced cardiac fibrosis depending on Nrf2 signal pathway. (A, B) Efficiency test of Nrf2 siRNA. Cardiac fibroblasts were transfected with negative control siRNA (NC) or Nrf2 siRNA, and the total protein of Nrf2 was determined by Western blot. Western blot analysis of (C, D) α-SMA, (E) CTGF (F) Collagen I, and (G) Collagen III protein expression in CFBs. (H) Immunofluorescent staining for α-SMA (green) and nuclear marker DAPI (blue) in CFBs. Results are presented as the mean ±SEM (* p<0.05 and ** p<0.01 vs. control; # p<0.05 and ### p<0.01 vs. ALD; & p<0.05 vs. OMT+ALD).

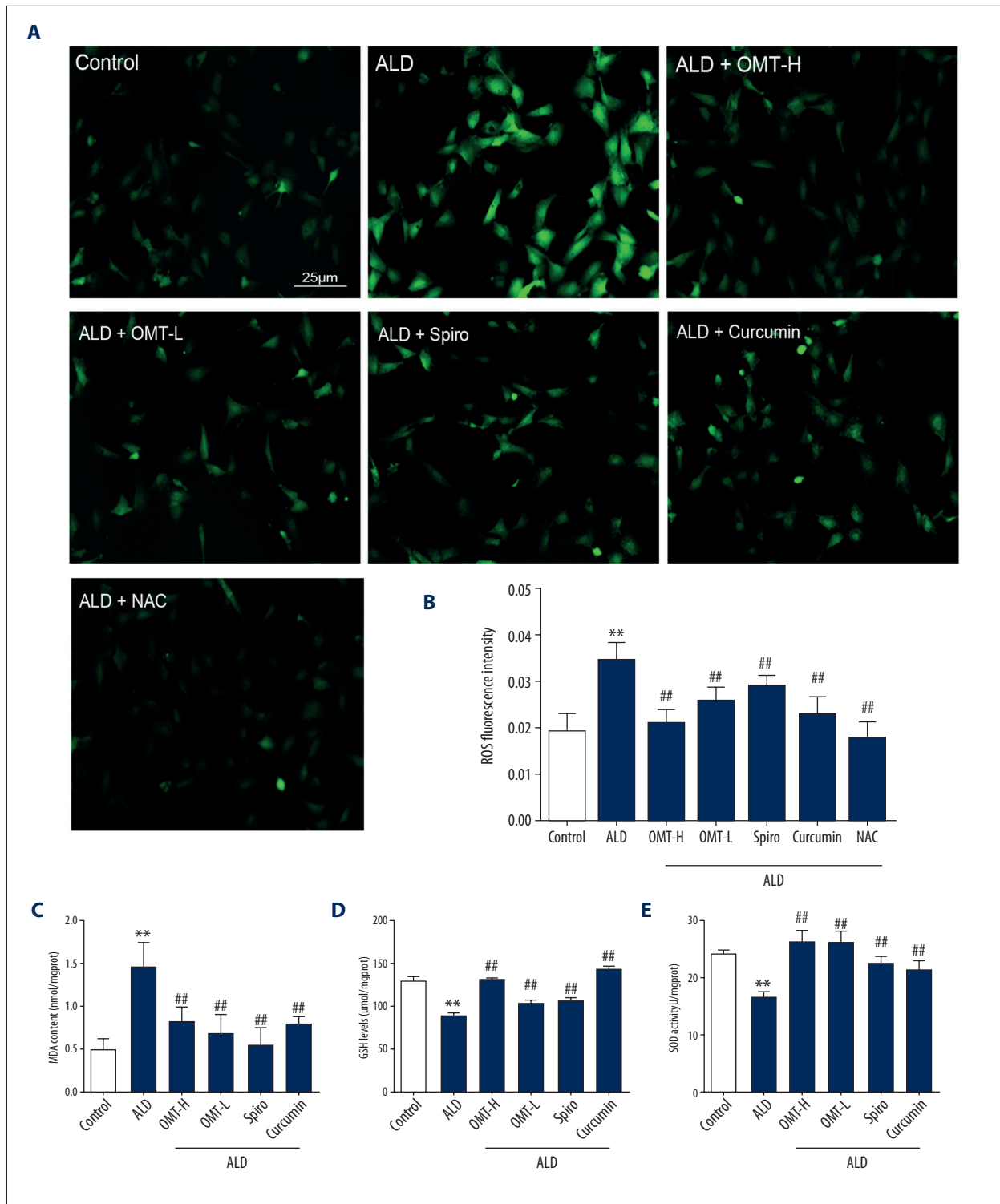


Figure 6. OMT and curcumin decreased oxidative stress levels in CFEBs induced by ALD. CFEBs were pretreated with 10 µmol/L curcumin, 1 µmol/L spironolactone (Spiro), 5 mmol/L N-acetylcysteine (NAC), 18.9 µmol/L OMT, or 37.8 µmol/L OMT for 2 h, and then exposed to 0.1 µmol/L ALD for 24 h. **(A)** Intracellular ROS were observed by fluorescence microscopy. **(B)** Quantitative analysis of intracellular ROS in CFEBs by fluorometry. The expression of **(C)** MDA, **(D)** GSH, and **(E)** SOD activity were determined by respective commercially available assay kit. Results are presented as the mean ± SEM (* p<0.05 and ** p<0.01 vs. control; # p<0.05 and ## p<0.01 vs. ALD).

fluorescence intensity of ROS increased significantly after CFBs were exposed to ALD. Pretreatment with OMT, spironolactone, and curcumin decreased the relative fluorescence intensity of ALD-induced ROS, as well as ROS scavenger N-acetylcysteine (NAC). Furthermore, malondialdehyde (MDA) is widely used as an oxidative stress marker. glutathione (GSH) and superoxide dismutase (SOD) protect cells from ROS damage as ROS scavengers. As shown in Figure 6C–6E, ALD exposed to CFBs, the level of MDA was significantly increased compared with the control group, and the GSH and SOD activity of CFBs was significantly decreased by ALD stimulation. Pretreatment with OMT, spironolactone, and curcumin significantly decreased the ALD-induced MDA increase and enhanced the ALD-reduced GSH level and SOD activity.

Discussion

We showed that OMT, MR antagonist spironolactone, and Nrf2 agonist curcumin can ameliorate transdifferentiation of cardiac fibroblasts to myofibroblasts induced by ALD *in vitro*. In CFBs exposed to ALD, OMT inhibited cardiac fibroblast-to-myoblast transformation and collagen production (collagen I and collagen III) in an Nrf2-dependent manner. Moreover, OMT, MR antagonist spironolactone, and Nrf2 agonist curcumin reduced ROS generation and MDA production, and increased anti-oxidative GSH levels and SOD activity. Furthermore, similar to curcumin, OMT activated and accelerated the translocation of Nrf2 to the nucleus.

Pathological cardiac fibrosis is involved in almost all the pathophysiological processes of cardiovascular diseases. Finding novel molecular targets to inhibit cardiac fibrosis in humans has been an important research focus. The main pathological characteristics of cardiac fibrosis are transdifferentiation, which enhances proliferation and myofibroblast differentiation of CFBs, and excessive ECM accumulation [24–26]. Aldosterone is a pivotal fibrosis factor of the renin-angiotensin-aldosterone system, which deteriorates cardiac oxidative stress and cardiac fibrosis, as well as activating MR. Increasing data suggest that MR activation exacerbates the pro-inflammatory/fibrotic effects of AngII-AT1R signaling by increasing cardiac oxidative stress. MR antagonists such as spironolactone have beneficial influences on cardiac remodeling and oxidative stress [27]. Studies have shown that amelioration of cardiac fibrosis in diabetic rats was possible through inhibiting oxidative stress [28]. Nrf2 is an antioxidant and a crucial factor in reducing oxidative stress [29]. Furthermore, Nrf2 knockdown abolished curcumin-alleviating CCl₄-induced hepatic fibrosis. Curcumin activates Nrf2 and promotes the translocation of Nrf2 to the nucleus and attenuates hepatic fibrosis [30]. We previously reported that OMT inhibits CFBs proliferation, differentiation, migration, and extracellular matrix

secretion [3,5,19] and ameliorates myocardial fibrosis induced by acute myocardial infarction in rats [31]. OMT ameliorates hepatic fibrosis induced by thioacetamide [32] and also inhibits oxidative stress [33]. OMT inhibits collagen synthesis in keloid fibroblasts and ameliorates bleomycin-induced lung fibrosis [34,35]. In the present study, we found that CFBs exposed to ALD induced proliferation and myofibroblast differentiation of CFBs, and then the Nrf2 agonists curcumin, Nrf2 siRNA, and OMT were used to evaluate changes.

The differentiation, proliferation, migration, and collagen deposition of fibroblasts play key roles in fibrosis [36,37]. In CFBs exposed to ALD, the proliferation and migration ability was significantly increased, whereas pretreatment with OMT, MR antagonist spironolactone, and Nrf2 agonist curcumin attenuated proliferation and migration ability. Furthermore, OMT and curcumin reduced the number of fibroblasts in S phase of the cell cycle following ALD stimulation, which is similar to the effect of spironolactone, a competitive antagonist of aldosterone. OMT intervention and activation of Nrf2 signaling inhibits CFBs proliferation by cell cycle arrest and migration.

The proliferation of CFBs and excessive ECM accumulation are the predominant pathological characteristics of cardiac fibrosis. In addition, collagen III, collagen I, and FN are the main ECM proteins, α -SMA is a hallmark of myofibroblast differentiation, and CTGF is a crucial pro-fibrotic factor [2,38,39]. Our results showed that ALD stimulation remarkably increased the levels of collagen I, collagen III, CTGF, FN, α -SMA, and MR expression, which were significantly depressed by pretreatment with OMT, spironolactone, and curcumin. Hyp, the decomposition product of collagen, is considered to be a biomarker of collagen quantity, which was quantified to evaluate the degree of cardiac fibrosis [40,41]. In CFBs exposed to ALD, the Hyp content was significantly increased in medium, whereas pre-incubation with OMT, spironolactone, and curcumin depressed the content. OMT, blockade of the MR, and activation of Nrf2 signaling can inhibit transdifferentiation of CFBs to myofibroblasts and collagen deposition, attenuating cardiac fibrosis induced by ALD.

Oxidative stress can promote the development of cardiac fibrosis, and the antioxidant N-acetylcysteine can attenuate cardiac fibrosis and heart failure in mice, possibly by reducing oxidative stress [42,43]. In the present study, OMT, spironolactone, and curcumin downregulated levels of ROS and MDA and upregulated levels of GSH and SOD activity in CFBs induced by ALD. Our data indicate that Nrf2 participates in the antioxidant effects of OMT, and the anti-fibrotic effect of OMT might occur by decreasing oxidative stress levels and promoting anti-oxidative GSH and SOD activity. Nrf2 is the key regulator of the antioxidant response and anti-fibrotic effects [44]. Our results suggest that ALD promotes the protein expression of Nrf2 and Keap1 in

cytoplasm, and decreases Nrf2 in the nucleus and HO-1 in CFBs, and these effects were reversed by OMT, spironolactone, and curcumin. OMT suppresses ALD-induced CFBs transdifferentiation and is related to the Nrf2/Keap1 signaling pathway. There was no significant difference in protein expression between the curcumin groups and the OMT+curcumin treated group, and qRT-PCR results show that pre-incubation with OMT, spironolactone, and curcumin increases the ALD-induced reduce the mRNA expression of Nrf2. These findings suggest that similar to the effects of curcumin, OMT activated and enhanced the expression of Nrf2 in the nucleus. Furthermore, we confirmed that the upregulated levels of collagen I, collagen III, α -SMA, and CTGF induced by ALD were significantly decreased by OMT, and Nrf2 siRNA abolished this reduction. Our results indicate that the anti-fibrotic effects of OMT on CFBs were Nrf2-dependent. Thus, OMT activates Nrf2 signaling, reducing cardiac fibrosis through the Nrf2 signaling pathway.

Conclusions

We investigated the OMT, activation of Nrf2 signaling, and inhibition of MR, which can suppress collagen synthesis, CFBs proliferation, and differentiation induced by ALD. OMT exerts

anti-fibrotic effects by activating Nrf2 signaling, suggesting that OMT prevents cardiac fibrosis and may be a potential therapeutic agent.

Conflicts of interests

None.

Abbreviations

CVDs – cardiovascular diseases; **CFBs** – cardiac fibroblasts; **OMT** – oxymatrine; **ALD** – aldosterone; **Spiro** – spironolactone; **ECM** – extracellular matrix; **α -SMA** – α -smooth muscle actin; **FN** – fibronectin; **CTGF** – connective tissue growth factor; **MR** – mineralocorticoid receptor; **ROS** – reactive oxygen species; **MMPs** – matrix metalloproteinases; **Nrf2** – nuclear factor-erythroid-2-(NF-E2)-related factor 2; **Keap1** – Kelch-like ECH-associated protein 1; **AREs** – antioxidant response elements; **HO-1** – heme oxygenase-1; **SOD** – superoxide dismutase; **GSH** – glutathione; **Hyp** – hydroxyproline; **FBS** – fetal bovine serum; **qRT-PCR** – quantitative real-time polymerase chain reaction; **DCFH-DA** – 2',7'-dichlorofluorescein diacetate; **DMSO** – dimethyl sulfoxide; **MTT** – 3-(4, 5-dimethylthiazol-2-yl)-2,5-diphenyltetrazolium bromide.

References:

1. Weiwei C, Runlin G, Lisheng L et al. Outline of the report on cardiovascular diseases in China, 2014. *Eur Heart J Suppl.* 2016;18: F2-F11
2. Wang C, Luo H, Xu Y et al: Salivianolic acid B-alleviated angiotensin II induces cardiac fibrosis by suppressing NF- κ B pathway *in vitro*. *Med Sci Monit*, 2018; 24: 7654–64
3. Xu Y, Xiao H, Luo H et al: Inhibitory effects of oxymatrine on TGF- β 1-induced proliferation and abnormal differentiation in rat cardiac fibroblasts via the p38MAPK and ERK1/2 signaling pathways. *Mol Med Rep*, 2017; 16(4): 5354–62
4. Rathod RH, Powell AJ, Geva T et al: Myocardial fibrosis in congenital heart disease. *Circ J*, 2016; 80(6): 1300–7
5. Zhao L, Xu Y, Tao L et al: Oxymatrine inhibits transforming growth factor β 1 (TGF- β 1)-induced cardiac fibroblast-to-myofibroblast transformation (FMT) by mediating the notch signaling pathway *in vitro*. *Med Sci Monit*, 2018; 24: 6280–8.
6. Tian J, An X, Niu L: [Myocardial fibrosis in congenital and pediatric heart disease (Review).] *Experimental and Therapeutic Medicine*, 2017; 13(5): 1660–64 [in Chinese]
7. Lee SW, Won JY, Kim WJ et al: Snail as a potential target molecule in cardiac fibrosis: Paracrine action of endothelial cells on fibroblasts through snail and CTGF axis. *Mol Ther*, 2013; 21(9): 1767–77
8. Bagchi RA, Roche P, Aroutiounova N et al: The transcription factor scleraxis is a critical regulator of cardiac fibroblast phenotype. *BMC Biology*, 2016; 14: 21
9. Sakamuri SS, Valente AJ, Siddesha JM et al: TRAF3IP2 mediates aldosterone/salt-induced cardiac hypertrophy and fibrosis. *Mol Cell Endocrinol*, 2016; 429: 84–92
10. Muñoz-Durango N, Vecchiola A, Gonzalez-Gomez LM et al: Review article modulation of immunity and inflammation by the mineralocorticoid receptor and aldosterone. *Biomed Res Int*, 2015; 2015: 652738
11. Zheng D, Dong S, Li T et al: Exogenous hydrogen sulfide attenuates cardiac fibrosis through reactive oxygen species signal pathways in experimental diabetes mellitus models. *Cell Physiol Biochem*, 2015; 36(3): 917–29
12. Bache RJ, Chen Y: Nox2-induced myocardial fibrosis and diastolic dysfunction: Role of the endothelium. *J Am Coll Cardiol*, 2014; 63(24): 2742–44
13. Bonsu KO, Owusu IK, Buabeng KO et al: Review of novel therapeutic targets for improving heart failure treatment based on experimental and clinical studies. *Ther Clin Risk Manag*, 2016; 12: 887–906
14. Cai SA, Hou N, Zhao GJ et al: Nrf2 is a key regulator on puerarin preventing cardiac fibrosis and upregulating metabolic enzymes UGT1A1 in rats. *Front Pharmacol*, 2018; 9: 540
15. Li X, Han D, Tian Z et al: Activation of cannabinoid receptor type II by AM1241 ameliorates myocardial fibrosis via Nrf2-mediated inhibition of TGF- β 1/Smad3 pathway in myocardial infarction mice. *Cell Physiol Biochem*, 2016; 39(4): 1521–36
16. Zhang YY, Yi M, Huang YP: Oxymatrine Ameliorates doxorubicin- induced cardiotoxicity in rats. *Cell Physiol Biochem*, 2017; 43(2): 626–35
17. Huang Y, Zhang J, Wang G et al: Oxymatrine exhibits anti-tumor activity in gastric cancer through inhibition of IL21R-mediated JAK2/STAT3 pathway. *Int J Immunopathol Pharmacol*, 2018; 32: 2058738418781634
18. Dai JP, Wang QW, Su Y et al: Oxymatrine inhibits influenza A virus replication and inflammation via TLR4, p38 MAPK and NF- κ B pathways. *Mol Sci*, 2018; 19(4): 965
19. Fu L, Xu Y, Tu L et al: Oxymatrine inhibits aldosterone-induced rat cardiac fibroblast proliferation and differentiation by attenuating smad-2, -3 and -4 expression: An *in vitro* study. *Complement Altern Med*, 2016; 16: 241
20. Xiao TT, Wang YY, Zhang Y et al: Similar to spironolactone, oxymatrine is protective in aldosterone-induced cardiomyocyte injury via inhibition of calpain and apoptosis-inducing factor signaling. *PLoS One*, 2014; 9(2): e88856
21. Wang HW, Shi L, Xu YP et al: Oxymatrine inhibits renal fibrosis of obstructive nephropathy by downregulating the TGF- β 1-Smad3 pathway. *Ren Fail*, 2016; 38(6): 945–51
22. Zhao HW, Zhang ZF, Chai X et al: Oxymatrine attenuates CCl₄-induced hepatic fibrosis via modulation of TLR4-dependent inflammatory and TGF- β 1 signaling pathways. *Int Immunopharmacol*, 2016; 36: 249–55
23. Gravez B, Tarjus A, Pelloux V et al: Aldosterone promotes cardiac endothelial cell proliferation *in vivo*. *J Am Heart Assoc*, 2015; 4: e001266
24. Li J, Zhang W, Jiao R et al: DIM attenuates TGF- β 1-induced myofibroblast differentiation in neonatal rat cardiac fibroblasts. *Int J Clin Exp Pathol*, 2015; 8(5): 5121–28

25. Li J, Dai Y, Su Z, Wei G: MicroRNA-9 inhibits high glucose-induced proliferation, differentiation and collagen accumulation of cardiac fibroblasts by down-regulation of TGFBR2. *Biosci Rep*, 2016; 36(6): e00417
26. Reeves SR, Kolstad T, Lien TY et al: Fibroblast-myofibroblast transition is differentially regulated by bronchial epithelial cells from asthmatic children. *Respir Res*, 2015; 16: 21
27. Mayyas F, Alzoubi KH, Van Wagoner DR: Impact of aldosterone antagonists on the substrate for atrial fibrillation: Aldosterone promotes oxidative stress and atrial structural/electrical remodeling. *Int J Cardiol*, 2013; 168(6): 5135-42
28. Zhang L, Mao Y, Pan J et al: Bamboo leaf extract ameliorates cardiac fibrosis possibly via alleviating inflammation, oxidative stress and apoptosis. *Biomed Pharmacother*, 2017; 95: 808-17
29. Xiao L, Xu X, Zhang F et al: The mitochondria-targeted antioxidant MitoQ ameliorated tubular injury mediated by mitophagy in diabetic kidney disease via Nrf2/PINK1. *Redox Biol*, 2017; 11: 297-311
30. Lu C, Xu W, Zheng S: Nrf2 activation is required for curcumin to induce lipocyte phenotype in hepatic stellate cells. *Biomed Pharmacother*, 2017; 95: 1-10
31. Shen XC, Yang YP, Xiao TT et al: Protective effect of oxymatrine on myocardial fibrosis induced by acute myocardial infarction in rats involved in TGF- β -Smads signal pathway. *J Asian Nat Prod Res*, 2011; 13(3): 215-24
32. Wu J, Pan L, Jin X et al: The role of oxymatrine in regulating TGF- β 1 in rats with hepatic fibrosis. *Acta Cir Bras*, 2018; 33(3): 207-15
33. Jiang G, Liu X, Wang M et al: Oxymatrine ameliorates renal ischemia-reperfusion injury from oxidative stress through Nrf2/HO-1 pathway. *Acta Circ Bras*, 2015; 30(6): 423-29
34. Fan DL, Zhao WJ, Wang YX et al: Oxymatrine inhibits collagen synthesis in keloid fibroblasts via inhibition of transforming growth factor- β 1/Smad signaling pathway. *Int J Dermatol*, 2012; 51(4): 463-72
35. Chen X, Sun R, Hu J et al: Attenuation of bleomycin-induced lung fibrosis by oxymatrine is associated with regulation of fibroblast proliferation and collagen production in primary culture. *Basic Clin Pharmacol Toxicol*, 2008; 103(3): 278-86
36. Guo J, Jia F, Jiang Y et al: Potential role of MG53 in the regulation of transforming-growth-factor- β 1-induced atrial fibrosis and vulnerability to atrial fibrillation. *Exp Cell Res*, 2018; 362(2): 436-43
37. Liu X, Song X, Lu J et al: Neferine inhibits proliferation and collagen synthesis induced by high glucose in cardiac fibroblasts and reduces cardiac fibrosis in diabetic mice. *Oncotarget*, 2016; 7(38): 61703-15
38. Wu D, Lei H, Wang JY et al: CTRP3 attenuates post-infarct cardiac fibrosis by targeting Smad3 activation and inhibiting myofibroblast differentiation. *J Mol Med (Berl)*, 2015; 93(12): 1311-25
39. Zhou H, Yu X, Zhou G: NLRC5 silencing ameliorates cardiac fibrosis by inhibiting the TGF- β 1/Smad3 signaling pathway. *Mol Med Rep*, 2017; 16(3): 3551-56
40. Yang J, Wu S, Zhu L et al: Hydrogen-containing saline alleviates pressure overload-induced interstitial fibrosis and cardiac dysfunction in rats. *Mol Med Rep*, 2017; 16(2): 1771-78
41. Wu X, Qi X, Lu Y et al: Liguzinediol protects against cardiac fibrosis in rats *in vivo* and *in vitro*. *Biomed Pharmacother*, 2016; 80: 260-67
42. Wang LP, Fan SJ, Li SM et al: Oxidative stress promotes myocardial fibrosis by upregulating KCa3.1 channel expression in AGT-REN double transgenic hypertensive mice. *Eur J Physiol*, 2017; 469(9): 1061-71
43. Giam B, Chu PY, Kuruppu S et al: N-acetylcysteine attenuates the development of cardiac fibrosis and remodeling in a mouse model of heart failure. *Physiol Rep*, 2016; 4(7): e12757
44. Prestigiacomo V, Suter-Dick L: Nrf2 protects stellate cells from Smad-dependent cell activation. *PLoS One*, 2018; 13(7): e0201044